

Searching for the continuum spectrum photons correlated to the 130 GeV γ -ray line

Ilias Cholis,^{1,2,*} Maryam Tavakoli,^{1,2,†} and Piero Ullio^{1,2,‡}

¹*SISSA, Via Bonomea, 265, 34136 Trieste, Italy*

²*INFN, Sezione di Trieste, Via Bonomea 265, 34136 Trieste, Italy*

(Dated: October 16, 2018)

Indications for a γ -ray line(s) signal towards the Galactic center at an energy of about 130 GeV have been recently presented. While dark matter annihilations are a viable candidate for this signal, it is generally expected that such a flux would be correlated to a γ -ray component with continuum energy spectrum due to dark matter pair annihilating into other Standard Model particles. We use the γ -ray data from the inner $10^\circ \times 10^\circ$ window to derive limits for a variety of DM annihilation final states. Extending the window of observation, we discuss bounds on the morphological shape of a dark matter signal associated to the line, applying both standard templates for the dark matter profile, such as an Einasto or a NFW profile, and introducing a new more general parametrization.

I. INTRODUCTION

Dark Matter (DM) accounts for approximately 85% of the matter density of the Universe. Among the many possible scenarios on its nature, Weakly Interacting Massive Particles (WIMPs) thermally produced in the early Universe are compelling candidates. WIMPs have a very rich phenomenology: they may be produced at colliders as the LHC, they may be detected by their direct interactions with baryonic matter or indirectly by singling out a component in cosmic rays and γ -rays due to their pair annihilation into Standard Model (SM) particles.

Among the possible signals of DM annihilation/decay, the search for a monochromatic γ -ray flux in multiple directions is one of the indirect detection methods with cleanest signature. As a prime target for such a signal, there is the galactic center (GC) direction, given that the annihilation/decay rate of DM in the halo peaks in that region.

Recently [1] has suggested the detection of a line at $129.8 \pm 2.4_{-13}^{+7}$ GeV with a 3.3σ significance in a wide window towards the GC. Additionally [2] has revealed an excess of γ -rays concentrated around the GC that, if modeled as a single line, is at 127.0 ± 2.0 GeV at 5.0σ significance. A pair of lines with energies of 110.8 ± 4.4 and 128.8 ± 2.7 GeV can also explain the excess of γ -rays with 5.4σ significance. Apart from the morphological differences these results agree on the energy of the line. Also both signals are in agreement with the constraints on line searches from the *Fermi* Collaboration [3]. Other authors have also suggested the presence of one [4] line at 130 GeV or multiple lines [5, 6] at $\simeq 110$ and 130 GeV towards the galactic center. The morphology of the line signal from both [1] and especially from [2] leads us to concentrate on DM annihilation rather than decay.

Most WIMP models that can give a line(s) signal do so with a production rate which is loop-suppressed. Typi-

cally the monochromatic γ -ray yield comes together with a γ -ray yield with continuum spectrum due to the annihilation, at tree-level, into other two-body SM final states, which in turn hadronize and/or decay into the stable species, p , \bar{p} , e^\pm , νs and γ -rays. Given that we have a preferred direction (inner few degrees of the GC) and a preferred mass range (correlated to the ~ 130 GeV line), for the DM explanation of the line(s), we can place specific limits on the continuous γ -ray component from DM annihilation (see for example [7, 8]). Alternative explanations for the line signal have also been suggested in [6, 9, 10].

In section II we describe our method of calculating limits on the continuous component for a variety of SM annihilation products. Additionally, using the γ -ray data in the energy range of the line(s) and assuming it is a DM signal we can study the morphology of events at that energy in the sky by extending our observation window. We show these results in section III. In section IV we implement our limits for a specific DM scenario and give our conclusions in section V.

II. EXTRACTING LIMITS ON DM ANNIHILATION FROM THE INNER $10^\circ \times 10^\circ$

In [2] the angular extension of the γ -ray line(s) signal at 110-130 GeV is described by a gaussian with FWHM of $3^\circ - 4^\circ$. If that signal comes from DM annihilation, the same region must be used to study the room for a γ -ray yield with continuum spectrum due to DM annihilation into other final states piling up at energies below 130 GeV. For that purpose we use the region of the inner $10^\circ \times 10^\circ$ box ($|b| < 5^\circ$, $|l| < 5^\circ$).

In this analysis we have calculated spectra using 3 years of *Fermi* LAT γ -ray data, taken between August 2008 and August 2011. Using the FermiTools PASS7 (v9r23p1) “ULTRACLEAN” class of data that ensures minimal CR contamination [31]. We bin all the γ -ray events with energies of 200 MeV and up to 500 GeV in 30 logarithmically spaced energy bins [32]. We separately calculate the exposures (and fluxes using HEALPix [11]) for front and back-converted events, before summing

*Electronic address: ilias.cholis@sissa.it

†Electronic address: tavakoli@sissa.it

‡Electronic address: ullio@sissa.it

their contribution to the total flux within the windows of interest.

To account for the contribution from known point and extended sources within the windows of interest we have used the 2 yr published catalogue (see [12] and references therein). Since we care to extract conservative limits on DM annihilation from γ -rays with energy below 130 GeV towards the inner $10^\circ \times 10^\circ$ we ignore the contribution of the *Fermi* Bubbles [13] / *Fermi* haze [14], [15]; given that there are significant uncertainties on the exact morphology of these structures at lower latitudes [15].

The γ -rays in the window of the inner $10^\circ \times 10^\circ$ originate from a combination of sources. There are 29 detected point sources centered in that window [12], 2 close by extended sources that contribute minimally [16, 17], as well as the diffuse γ -rays from inelastic collisions of CRs with the interstellar medium (ISM) gas, from bremsstrahlung radiation off CR electrons and from up-scattering of low energy photons of the interstellar radiation field (ISRF) from high energy CR e (inverse Compton scattering). Additionally many unknown dim point sources are expected to be located within that window. Finally the possible γ -ray contribution from DM annihilations in the halo is expected to peak towards the galactic center.

These γ -rays can be the direct product of DM annihilations as in the case of the monochromatic yield from the 2γ , $Z\gamma$ or $h\gamma$ final states, possibly matching the lines detected by [1, 2]. Also virtual internal bremsstrahlung (VIB) and final state radiation (FSR) in DM annihilation can give a very hard spectrum that can be confused as a line over an otherwise featureless power law spectrum [10, 18]. The decay of mesons (predominantly π^0 s), produced in the decay or hadronization processes of the products of DM annihilation, can also lead to a significant contribution to the gamma-ray spectrum. This component, while typically harder than the background γ -ray spectra, is significantly softer than the VIB/FSR and can not be confused as a DM line in γ -rays. These contributions probe directly the DM annihilation profile and will be referred to, as prompt γ -rays. Additionally, inverse Compton and bremsstrahlung γ -rays from the leptonic final products (e^\pm) of DM annihilation will also contribute in that window since both the ISRF energy density and the ISM gas density peak in the inner part of the Galaxy.

As we suggested in the introduction, we will concentrate only on the DM annihilation case since the line(s) morphology is so confined that it favors profiles of cuspy annihilating DM halos (see also our discussion in section III).

To compute the diffuse γ -ray background we use the DRAGON package [19, 20] [21] with a new ISM gas model [22] that ensures good agreement with γ -ray data in that window and overall [23]. We ignore in this work the contribution from the dark gas whose uncertainties are though significant in the inner 5° in latitude [24, 25] but that would only add to the diffuse γ -ray background resulting in less room for DM annihilation originated γ -

rays.

We study five individual modes/channels of DM annihilation: $\chi\chi \rightarrow W^+W^-$, $\chi\chi \rightarrow b\bar{b}$, $\chi\chi \rightarrow \tau^+\tau^-$, $\chi\chi \rightarrow \mu^+\mu^-$ and $\chi\chi \rightarrow e^+e^-$. Typically, DM models have sizable branching ratios into more than one of these channels. The exact limits in such models can be recovered by linearly combining the limits from the above channels. Annihilations to Z gauge bosons give very similar γ -ray spectra to those of W^+W^- bosons and annihilations to top quarks -not on shell in these cases- similar γ -ray spectra of annihilations to b quarks. Thus the constraints to those channels can be taken to be the same (within $\simeq 10\%$) to those of the $\chi\chi \rightarrow W^+W^-$ ($\chi\chi \rightarrow b\bar{b}$).

Following [2] we assume that a line at energy of 127 ± 2 GeV has been detected. The morphology of the excess is described by a bi-gaussian with FWHM of 4 degrees in both l and b . That line can come from $\chi\chi \rightarrow 2\gamma$ or $\chi\chi \rightarrow Z\gamma$ or $\chi\chi \rightarrow h\gamma$. In [1] a single line at $129.8 \pm 2.4^{+7}_{-13}$ GeV has been suggested. Additionally the case where there are 2 lines centered at 128.8 ± 2.7 and 110.8 ± 4.4 GeV has been indicated by [2]. In that case the lines come from either the combination of 2γ & $Z\gamma$ lines or from the $Z\gamma$ & $h\gamma$ lines.

We study both the case of a single line centered at 127 GeV and the case of 2 lines centered at 129 and 111 GeV. The choice of mass depends on the exact origin of the line(s). For a single line from $\chi\chi \rightarrow 2\gamma$ the mass range of $122 < m_\chi < 132$ GeV is studied. For a single line from $\chi\chi \rightarrow Z\gamma$ we study $137 < m_\chi < 145$ GeV and from $\chi\chi \rightarrow h\gamma$ we study the $149 < m_\chi < 157$ GeV mass range. For 2 lines originating from 2γ & $Z\gamma$ we study $127 < m_\chi < 130$ and for the case of $Z\gamma$ & $h\gamma$ lines $138 < m_\chi < 143$ GeV (for a two line signal from DM annihilation see also [26]). The relevant ratio in the luminosity of the two lines is taken to be 0.7/1 for the 111/129 GeV lines. We allow for 4% uncertainty in the determination of energy of the line(s) which leads to the ranges of masses referred above, which is about 2σ of the declared uncertainties of [2] and [1] [33].

For every choice of annihilation channel to continuum γ -rays, annihilation channel(s) to line(s) and DM mass, we first find the best fit values from the γ -ray data within $10^\circ \times 10^\circ$ for both the cross-section of the main annihilation channel (giving the continuum γ -rays) and separately for the annihilation cross-section to the line(s) (2 d.o.f.).

In Fig. 1, we show a fit to the total γ -ray spectrum within our window of interest for the case of $\chi\chi \rightarrow W^+W^-$, with $m_\chi = 130$ and a single line coming from $\chi\chi \rightarrow 2\gamma$. The fact that the best fit value for the cross-section is positive validates our claim of deriving conservative limits on DM annihilation, while the good agreement to the low ($E_\gamma < 1$ GeV) energies where the DM contributes at the few % level shows the good agreement of the physical model for the background to the low energy data.

From the best fit value we then derive the 3σ upper limits of the main annihilation channel keeping the an-

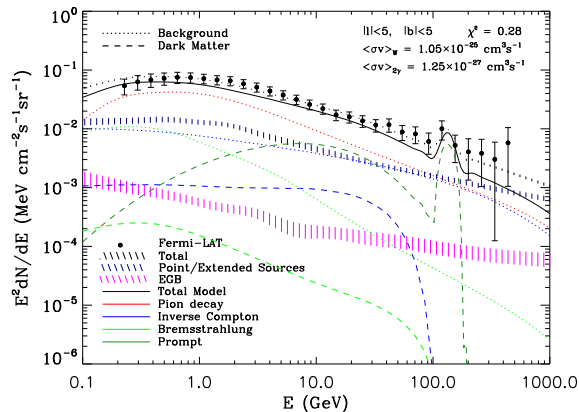


FIG. 1: Case of $m_\chi = 130$ GeV DM particle annihilating to a W^+W^- pair with a cross-section of $1.05 \times 10^{-25} \text{ cm}^3 \text{ s}^{-1}$ and to a 2γ line with a cross-section of $1.25 \times 10^{-27} \text{ cm}^3 \text{ s}^{-1}$. We plot the $|b| < 5^\circ, |l| < 5^\circ$.

nihilation to the line fixed to its best fit value. In Fig. 2 we show these 3σ upper limits for the five annihilation channels to W^+W^- , $b\bar{b}$, $\tau^+\tau^-$, $\mu^+\mu^-$ and e^+e^- . We show limits for both the case of a single line Fig. 2 (top left) and for a double line Fig. 2 (top right). The exact choice of the origin of the line(s) and its energy(ies) has a subdominant effect on the limits in all channels except in the case of e^+e^- . That happens since the DM contribution of the main channel to the γ -ray spectrum is at energies below 100 GeV where the lines do not contribute. The case of the e^+e^- channel is an exception due to the very significant FSR component which peaks at m_χ . Thus the FSR component competes with the line(s) in the fit, making its limits sensitive to the exact assumptions on the line(s). We also give in Fig. 2 (bottom panels) the best fit values for the line(s) for the relevant combinations of DM mass and channel.

The ISRF photon and gas densities have been fixed based on our background model. The assumptions on these densities influence the inverse Compton and bremsstrahlung components respectively. One can derive even more conservative limits on the DM annihilation channels by considering only the prompt γ -ray contribution.

In Fig. 3 we give the 3σ limits where only the prompt γ -rays from DM are taken into account. For the W^+W^- , $b\bar{b}$ and $\tau^+\tau^-$ channels, for which the prompt γ -rays are the dominant component, the limits become weaker only by $\simeq 10 - 20\%$. For the $\mu^+\mu^-$, e^+e^- modes on the contrary, since hard CR electrons are injected, their inverse Compton and bremsstrahlung components are significant. Thus if we ignore these diffuse components keeping only the prompt component, the 3σ limits become weaker by a factor of 4-5 in both channels.

The limits shown in Figs. 2 and 3 depend on the DM

profile assumptions. We use here an Einasto DM profile:

$$\rho(r) = \rho_{Ein} \exp \left[-\frac{2}{R_c} * \left(\frac{r^\alpha}{R_c^\alpha} - 1 \right) \right], \quad (1)$$

with $\alpha = 0.22$, $R_c = 15.7$ kpc and ρ_{Ein} is set such that the local DM density is equal to 0.4 GeV cm^{-3} [27, 28]. That results in a J-factor from that window of $J/\Delta\Omega = 1.21 \times 10^{24} \text{ GeV}^2 \text{ cm}^{-5}$, where J factor is defined here as:

$$J = \int_{\Delta\Omega} \int_0^\infty \rho_{DM}^2(s, \Omega) ds d\Omega, \quad (2)$$

with s to be the distance along line of sight and $\Delta\Omega$ the angle of observation.

A more cuspy DM profile would lead to stronger limits while a more cored (flat) in the inner kpcs would lead to weaker limits. All the limits shown in Fig. 3 and the limits for W^+W^- , $b\bar{b}$ and $\tau^+\tau^-$ in Fig. 2 will change inverse proportionally (exactly or approximately) to the value of the J-factors within that window, since the prompt component is dominant in these channels. The same applies for the best fit values to the line(s). Thus these limits can be used for other DM profile assumptions once one properly takes into account the different J-factor from that window. For the annihilation channels into $\mu^+\mu^-$ and e^+e^- the limits in Fig. 2 have a dependence on the DM profile that is more involved.

Finally since our aim in this paper is not to study the line itself but the accompanying γ -ray fluxes for the DM case, we want to ensure that the exact line assumptions that we make do not influence our limits for the continuous component. The 3σ limits presented in Figs.2 and 3 were derived with the cross-section to the line(s) to be the best fit value from the fit to the γ -ray data within $|l| < 5^\circ, |b| < 5^\circ$. Alternatively, we calculate the 3σ limits for the same channels using for the cross-section to the line(s) such a value that gives the luminosity stated for the 4° FWHM cusp of [2], that is $(1.7 \pm 0.4) \times 10^{36} \text{ ph/s}$ or $(3.2 \pm 0.6) \times 10^{35} \text{ erg/s}$. The difference in the values of the cross-sections to the line(s) between the two methods is $\simeq 30\%$ (at the same level with the stated uncertainty of [2]).

In Table I we present our limits *on the continuous components* for these two alternative methods of evaluating the cross-section to the line(s) before deriving the limits. For the case where the cross-section value to the line(s) comes from the $|l| < 5^\circ, |b| < 5^\circ$ region fit, (denoted as “free”) and for the case where the cross-section comes from the luminosity stated by [2]. We show all five channels for three masses characteristic for the three DM mass ranges valid in the case of a single line at 127 GeV.

The difference in the limits for all five channels and all masses between the two methods is at the $\simeq 1\%$ level. The same results apply for the case of 2 lines (111 and 129 GeV). Thus the exact luminosity assumptions for the line(s) can not influence our results on the continuous component.

We also find that changing our window of observation from $(|l|, |b|) < 5^\circ$, to $(|l|, |b|) < 3^\circ, 4^\circ$ or 8°

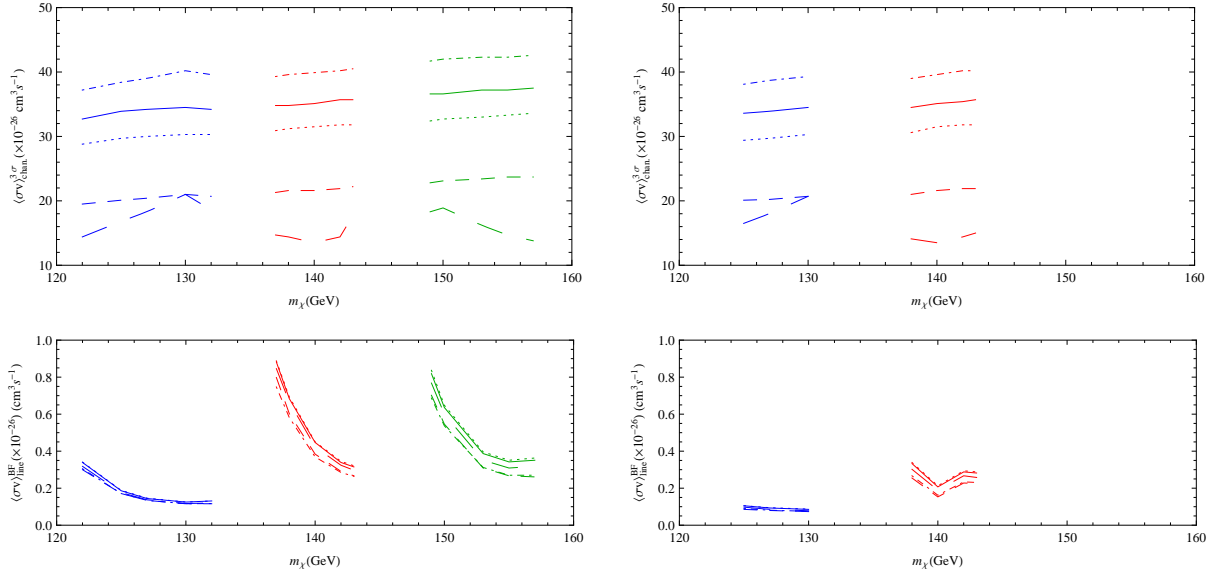


FIG. 2: Top: 3σ limits for annihilation into “channel”, from region of $|b| < 5^\circ$, $|l| < 5^\circ$. We study five channels. $\chi\chi \rightarrow W^+W^-$: solid lines, $\chi\chi \rightarrow b\bar{b}$: dotted lines, $\chi\chi \rightarrow \tau^+\tau^-$: dashed lines, $\chi\chi \rightarrow \mu^+\mu^-$: dashed dotted lines and $\chi\chi \rightarrow e^+e^-$: long dashed lines. Left: assuming a single line from $\chi\chi \rightarrow 2\gamma$ (blue), or $\chi\chi \rightarrow Z\gamma$ (red) or $\chi\chi \rightarrow h\gamma$ (green). Right: assuming double lines from $\chi\chi \rightarrow 2\gamma$ and $\chi\chi \rightarrow Z\gamma$ (blue), from $\chi\chi \rightarrow Z\gamma$ and $\chi\chi \rightarrow h\gamma$ (red). Bottom: best fit values for the annihilation into line(s). For the double line case the annihilation best fit value refers to the cross-section for the highest energy line; the 111/129 GeV luminosity ratio is taken to be 0.7/1. We use the Einasto DM profile of eq. 1 which gives $J/\Delta\Omega = 1.21 \times 10^{24} \text{ GeV}^2 \text{ cm}^{-5}$ (see text for more details).

Chan.	Line	127 GeV (2γ)	140 GeV ($Z\gamma$)	150 GeV ($h\gamma$)
W^+W^-	Free	34.2(40.8)	35.1(42.6)	36.6(44.1)
W^+W^-	Fixed	34.5(41.4)	35.4(43.2)	37.2(44.7)
$b\bar{b}$	Free	30.0(31.5)	31.5(33.3)	32.7(34.5)
$b\bar{b}$	Fixed	30.3(31.8)	31.8(33.6)	33.0(34.8)
$\tau^+\tau^-$	Free	20.4(21.9)	21.6(23.4)	24.1(24.9)
$\tau^+\tau^-$	Fixed	20.7(21.9)	21.9(23.7)	23.4(25.2)
$\mu^+\mu^-$	Free	39.0(155.7)	39.9(169.8)	42.0(185.4)
$\mu^+\mu^-$	Fixed	41.1(156.3)	40.2(167.7)	42.3(184.5)
e^+e^-	Free	18.3(91.8)	13.5(100.8)	18.9(111.0)
e^+e^-	Fixed	18.3(92.1)	13.5(99.3)	19.2(110.4)

TABLE I: 3σ upper limits on DM annihilation $\langle\sigma v\rangle \times BR$ to channel (i.e the continuum part) in units of $\times 10^{-26} \text{ cm}^3\text{s}^{-1}$ using full (in parenthesis:only prompt) DM γ -ray spectra within $|l| < 5^\circ$, $|b| < 5^\circ$. The line signal is taken to be either from its best fit value (free) or fixed using the luminosity of [2] (see text for more details). The J -factor/ $\Delta\Omega$ from this window is $1.21 \times 10^{24} \text{ GeV}^2 \text{ cm}^{-5}$.

our limits for the continuous component (for the best fit value for the line(s)) change by up to 10% (20%), with the limits from $(|l|, |b|) < 5^\circ$ being the strongest (see also work of [5, 29]).

III. DARK MATTER ANNIHILATION SIGNAL PROFILE

Ref. [2], suggests that the line(s) signal can be morphologically fitted by a 4° FWHM gaussian distribution or 3° FWHM when using just the events and avoid making diffuse maps or masking out any part of the GC. The author of [1] has suggested instead a wider region of best significance for the 130 GeV line.

Using ULTRACLEAN data class we address as well the matter of DM profile morphology under the assumption that the line signal is of DM origin and that an associated continuous spectrum exists.

Calculating the γ -ray spectral data within a wider region of the sky we can derive limits on the allowed annihilation cross-section for a specific assumption on the DM halo profile or vice versa for the DM halo profile properties for specific assumptions on the annihilation cross-section.

Motivated by the $\simeq 130$ GeV energy of the γ -ray line, we consider a DM mass of $m_\chi = 130$ GeV annihilating to W^+W^- , with a cross-section to 2γ for the line.

We calculate the γ -ray spectra in the same energy binning as for the $10^\circ \times 10^\circ$ box described in section II. We concentrate in the $|b| < 25^\circ$, $|l| < 25^\circ$ region where the annihilation from the halo is dominant. We break that

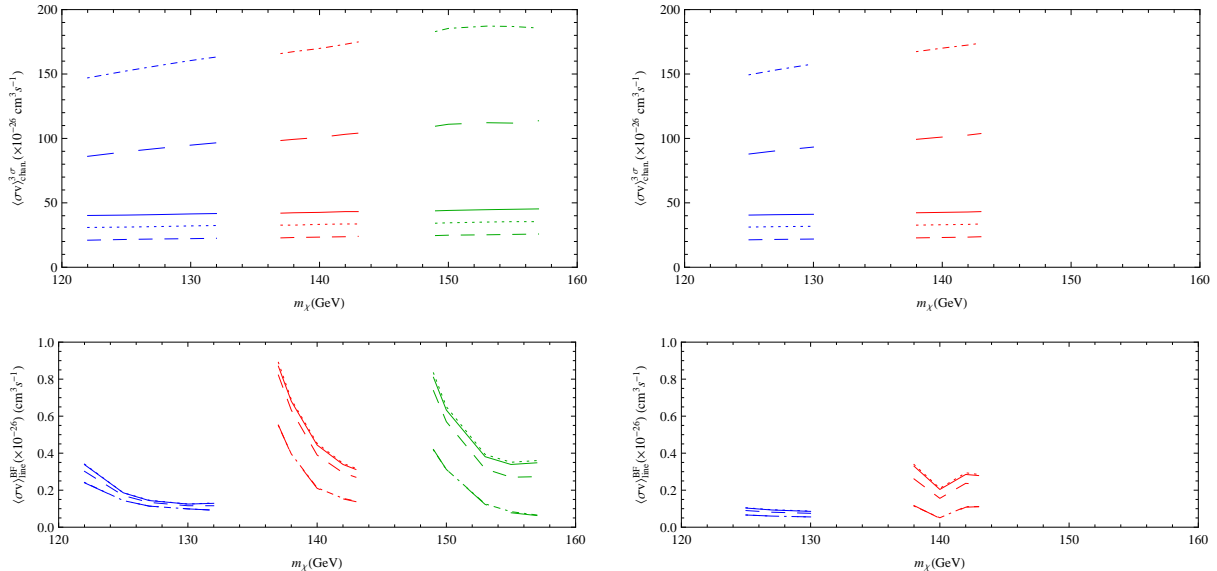


FIG. 3: Top: 3σ limits for annihilation into "channel" using only the prompt γ -rays from DM annihilation. We use the region of $|b| < 5^\circ$, $|l| < 5^\circ$. Left: assuming a single line. Right: assuming double lines. Lines and colors as in Fig. 2. Bottom: best fit values for the annihilation into line(s). We use the Einasto DM profile of eq. 1.

region in 20 smaller windows, 8 of which in the region $|b| < 10^\circ$, $|l| < 10^\circ$ of 5° size in l and 10° size in b . For $|b| > 10^\circ$, $|l| > 10^\circ$, 12 windows symmetrically placed with respect to $b = 0^\circ$, $l = 0^\circ$ each composed of 4 boxes $5^\circ \times 5^\circ$ size. These windows are also shown in Fig. 4.

In Fig. 4, we assume the DM profile to be either an Einasto as described in eq. 1, (Fig. 4, left panel) or an NFW profile (Fig. 4, right panel):

$$\rho(r) = \rho_{NFW} \left(\frac{R'_c}{r} \right) \left(\frac{1}{1 + \frac{r}{R'_c}} \right)^2, \quad (3)$$

with $R'_c = 14.8$ kpc, $\rho_{NFW} = 0.569$ GeV cm^{-3} . For both cases we fit the DM density to the locally measured value of 0.4 GeV cm^{-3} [27]. That results in a specific J-factor for each window.

We calculate as in section II the 3σ limits on $\chi\chi \rightarrow W^+W^-$ from each angular window. These limits include γ -ray background contribution that as in the $10^\circ \times 10^\circ$ box fits the lower energies.

In Fig. 4 we give the ratios of the 3σ limit on each window divided by the 3σ limit from the window of $-5^\circ < l < 0^\circ$, $|b| < 5^\circ$:

$$\frac{\langle \sigma v \rangle_{window}^{3\sigma}}{\langle \sigma v \rangle_{-5^\circ < l < 0^\circ, |b| < 5^\circ}^{3\sigma}}. \quad (4)$$

Values of the ratio in eq. 4 smaller than 1 indicate stronger 3σ limits than that in the window of reference. We choose the window of $-5^\circ < l < 0^\circ$, $|b| < 5^\circ$ as

reference since -as also thoroughly discussed in [2]- the majority of photons with energy ~ 130 GeV come from that part. We find 38 photons with energy $104.5 - 135.7$ GeV (the one energy bin in our analysis that includes the line(s)) to come from the $-5^\circ < l < 0^\circ$, $|b| < 5^\circ$ window, while only 21 photons in the same energy bin come from the symmetrical to the GC, $0^\circ < l < 5^\circ$, $|b| < 5^\circ$ window.

In our simulations the DM halo profile is centered at $l = 0^\circ$, $b = 0^\circ$. We find that our 3σ limits are stronger from the $0^\circ < l < 5^\circ$, $|b| < 5^\circ$ window than from the $-5^\circ < l < 0^\circ$, $|b| < 5^\circ$ one. We remind that these limits come from the continuous component (see discussion in section II), thus there is an indication even from the continuous DM component that there is an excess of γ -ray fluxes from the $l < 0$ side. That is seen with both the Einasto and NFW profiles.

We do not claim that such an excess is due to DM annihilations since it could equally correspond to an underestimation of the background in that energy range. Though that can be the case also for the line [6, 9]. Yet, if the line is of DM origin and is off-center as suggested by [2], the strength of the derived limits may indicate an analogous effect in the continuum term.

Once we move to $|l| > 5^\circ$ and $|b| < 5^\circ$ the strength of the 3σ limits drops. For the Einasto profile the limits become stronger at $-10^\circ < l < 5^\circ$, $5^\circ < |b| < 10^\circ$ and weaker in all other windows. For the more centrally peaked NFW profile the only region where slightly stronger limits are recovered is that of $-5^\circ < l < 0^\circ$,

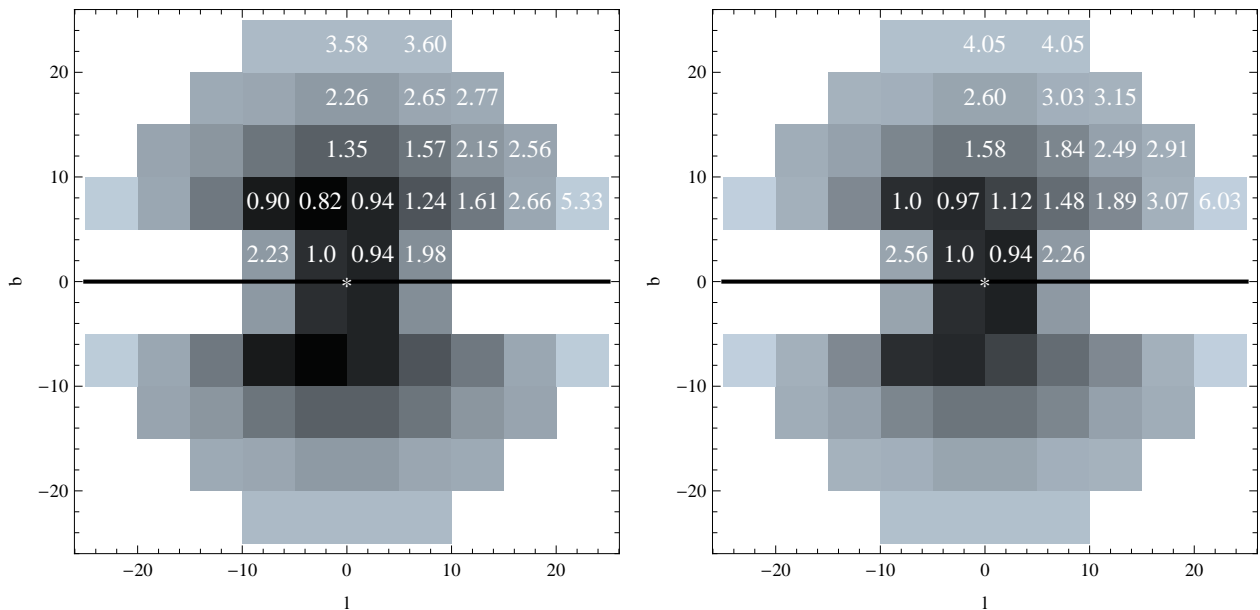


FIG. 4: Strength of limits on the annihilation cross-section to W^+W^- . Left: Einasto profile. Right: NFW profile. Values are normalized to the 3σ limit on the annihilation cross-section of $\chi\chi \rightarrow W^+W^-$ from $-5^\circ < l < 0^\circ$, $|b| < 5^\circ$ ($\langle\sigma v\rangle_{-5^\circ < l < 0^\circ, |b| < 5^\circ}^{3\sigma} = 3.72 \times 10^{-25} \text{cm}^3 \text{s}^{-1}$). Values smaller than 1 indicate stronger(lower) 3σ limit by the given (multiplication) factor.

$5^\circ < |b| < 10^\circ$.

Turning the perspective around, we discuss now what information can be extracted on the dark matter profile, having fixed the annihilation cross section to a reference value. Rather than introducing for the dark matter density some functional form specified in terms of few parameters, as most usually done in the literature, we consider here a much more general approach. Our generic spherically symmetric profile is set via: *i*) Specifying its value ρ_i at the seven Galactocentric distances $r_i = R_0 \sin(\alpha_i)$, being R_0 the Sun Galactocentric distance and with $\alpha_i = 5^\circ, 10^\circ, 15^\circ, 20^\circ, 25^\circ, 45^\circ$ & 65° , namely at the spherical shell corresponding to the angular windows already introduced above, plus three higher latitude patches; *ii*) Fixing the dark matter density at the local Galactocentric distance $r_8 \equiv R_0$ to $\rho_8 \equiv 0.4 \text{ GeV cm}^{-3}$ and implementing a linear interpolation in a double logarithmic scale to retrieve the density profile between any two of these radii, i.e. allowing for an arbitrary power-law scaling between any two r_i , with the only extra assumption of imposing that the profile is monotonically increasing for decreasing radius; *iii*) Assuming that the profile follows our reference Einasto model for $r > R_0$, a choice that has no impact on the analysis that follows.

We refer again to the sample dark matter case introduced in Fig. 1, with $m_\chi = 130 \text{ GeV}$ and annihilating to W^+W^- . While the ratio between the cross section into 2γ to the one into W^+W^- is fixed by the best fit value (in the specific case we found it to be about 0.012), the absolute value of the cross section scales with the inverse of the line of sight integration factor J in the angular window $|b| < 5^\circ$, $|l| < 5^\circ$, in turn depending on the

density profile within all the angular shells introduced above. After choosing a reference value for $\langle\sigma v\rangle$, we wish to derive how large a contribution to J may come from each of the shells in our model, without violating the constraints coming from data in other angular windows. This gives an indication on how centrally concentrated the dark matter profile should be to provide a signal in the GC direction and, at the same time, to be consistent with data away from it. For this purpose we introduce the factors J_i which are analogous to the J -factor introduced in Eq. 2, except for imposing that the density profile is constant below the radius r_i , namely $\rho(r < r_i) = \rho_i$.

The analysis is performed scanning the parameter space defined by the values ρ_i (with $i \in [1, 7]$). For each model we compute line of sight integration factors corresponding to the angular regions displayed in Fig. 4, as well as for the regions at $25^\circ < |b| < 45^\circ$, $45^\circ < |b| < 65^\circ$ and $65^\circ < |b| < 85^\circ$, and $0^\circ < |l| < 20^\circ$ (for all three latitude intervals). For all regions we can compare against the 3σ upper bound on the flux due to a dark matter candidate with mass 130 GeV and annihilating to W^+W^- (conservatively including prompt emission only, while ignoring the radiative emission from the associated lepton yields). As upper bound to the monochromatic signal we consider instead the mean flux integrated in the energy bin $[104.5, 135.7] \text{ GeV}$, obtained again using the ULTRACLEAN data sample, and under the very conservative hypothesis of zero background from diffuse emission. Among models passing constraints, we search for configurations giving the maximum for the individual terms J_i (we also implement the additional limit $J_1 \leq J$, given that any additional contribution to the line of sight inte-

gral at radii $r < r_1$ is always neglected in our setup). Although we are dealing with a very large parameter space, finding the upper bounds to J_i , which we label J_i^{max} , is not exceeding expensive since one can show that, for each radial shell, they mostly correspond to the models with largest changes in profile slope between neighboring shells.

Ratios between J_i^{max} and J are shown in Fig. 5, where we display separately the J_i^{max} found when applying the limit on the monochromatic flux and when implementing that from the component with continuum spectrum; limits are shown as (very narrow) bands since they were derived for three different values for $\langle\sigma v\rangle$: the “thermal” value $3 \times 10^{-26} \text{ cm}^3 \text{ s}^{-1}$, the best fit value in case of our reference Einasto profile $1.05 \times 10^{-25} \text{ cm}^3 \text{ s}^{-1}$, and ten times the thermal value (this shows that dependence of our analysis on $\langle\sigma v\rangle$ is really very mild). For comparison, we plot also values of J_i/J for our reference Einasto profile and for a Burkert profile, namely $\rho \propto 1/(r+R_c)/(r^2+R_c^2)$, with local dark matter density 0.4 GeV cm^{-3} and core radius $R_c = 10 \text{ kpc}$ [27]. As one can see the Burkert profile is excluded from both line and continuum components, while the line limits are giving stronger evidence towards the need for a more centrally concentrated dark matter profile. This is most probably related to the fact that the limits are derived in part from regions of the sky where the *Fermi* Bubbles/haze, has been claimed to be needed; we do not try to include such component in our background model and most probably this translates into an extra room (or a less severe constraint) on the continuum emission from dark matter annihilations. On the other hand, the *Fermi* Bubbles/haze are expected to play a marginal role at high energy, hence the sharper constraint from the line emissivity.

IV. A SPECIFIC EXAMPLE

The limits that we show in Fig. 2 and 3 can be used (linearly combined) for a wide class of models. As a specific example we use our code to evaluate the constraints on a relevant model presented for the explanation of a 130 GeV line [30].

In [30] the DM is composed by Winos and Axions at about equal amounts in DM mass density towards the GC. Following [30] we take the DM mass density in Winos to be 49% of the total in the GC and in the entire Galaxy. Using the Einasto model of eq. 1 we take DM mass to be $m_\chi = 145 \text{ GeV}$ and the cross-section to $Z\gamma$ line to be 1.26×10^{-26} . The total annihilation cross-section of the Winos is $3.2 \times 10^{-24} \text{ cm}^3 \text{ s}^{-1}$ and is dominantly to W^+W^- . Assuming a $\text{BR}=0.96$ for annihilation to W^+W^- we derive that such a model is excluded as we show in Fig. 6. In fact such a cross-section is $O(10)$ larger than the relevant 3σ limit for that mass and channel shown in Fig. 2.

We note that even ignoring the inverse Compton and bremsstrahlung components and all the background con-

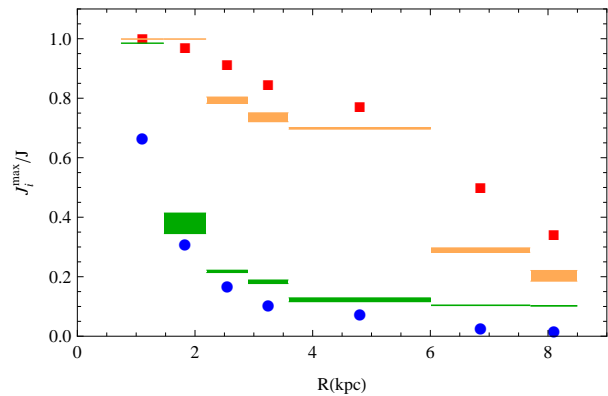


FIG. 5: Upper bounds on the partial J_i factor, normalized to the total GC line of sight integration factor J , for the parametric dark matter density profile introduced in the text. The J_i factor are computed assuming a constant dark matter density within the corresponding radial shell r_i . The J_i^{max} values displays are derived implementing separately the limits on the monochromatic flux (lower green bands) and the continuum spectrum (higher orange bands) derived from the other angular windows considered in the analysis. Limits are shown as narrow bands since they refer to three different values of the annihilation cross section, see the text for details. Also shown are the values for J_i/J for our reference Einasto profile (blue dots) and for a cored Burkert profile (red squares); as it can be seen the Einasto profile is allowed, while the Burkert shape is excluded.

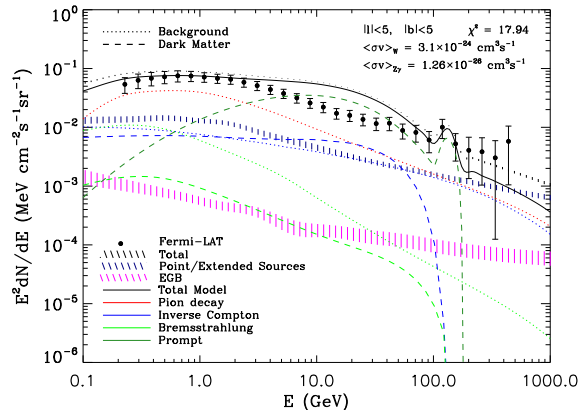


FIG. 6: Wino/Axion model of [30]. $m_\chi = 145 \text{ GeV}$ $\langle\sigma v\rangle_{\chi\chi \rightarrow Z\gamma} = 1.26 \times 10^{-26} \text{ cm}^3 \text{ s}^{-1}$, $\langle\sigma v\rangle_{\chi\chi}^{tot} = 3.2 \times 10^{-24} \text{ cm}^3 \text{ s}^{-1}$.

tribution, the prompt component which also includes the line signal overshoots the total γ -ray spectrum between 10 and 40 GeV. This result can not depend on just a different assumption for the DM profile or on a varying ratio in Wino to Axion mass density within the Galaxy since by changing any of these assumptions the γ -ray line will decrease/increase by the same amount.

V. CONCLUSIONS

Inspired by recent indications for a monochromatic γ -ray signal towards the GC, possibly connected to DM annihilations, we have derived limits on the continuous component that in general accompanies such signal. We use the region at $|l| < 5^\circ$, $|b| < 5^\circ$ and compute 3σ upper limits for DM annihilation cross-sections into the W^+W^- , $b\bar{b}$, $\tau^+\tau^-$, $\mu^+\mu^-$ and e^+e^- channels.

We derive limits both from the total DM γ -ray emission, including the prompt, the inverse Compton and the bremsstrahlung components as given in Fig. 2, and only from prompt DM γ -rays (given in Fig. 3). These limits do not depend on the exact normalization of the line(s) since they are dominated by the γ -ray data below 100 GeV, where the lines do not contribute (see Table I). While our limits depend on the choice of the DM halo profile, they can be easily rescaled to a different halo configuration. This happens since, apart from the $\mu^+\mu^-$ and e^+e^- channels, the prompt γ -rays are the dominant component.

We study the γ -ray data from other angular windows of the Galaxy and find that for cuspy DM profiles such as the NFW profile, the most stringent constraints come from our $|l| < 5^\circ$, $|b| < 5^\circ$ window while for the

Einasto profile slightly stronger limits can come from $5^\circ < |b| < 10^\circ$ (see Fig. 4). We have also introduced a new general parametrization for the DM profile to discuss how centrally concentrated the profile should be to give a flux compatible with the suggested GC line signal without violating bounds from other angular windows. We produced results for partial line-of-sight integration factors which are readily applicable to any dark matter profile, showing e.g. that a Burkert DM halo cannot be compatible (see Fig. 5).

Our limits on specific DM annihilation channels can be linearly combined and readily applied to most DM models in this mass range. We apply our limits to the model of [30] and conclude that it is excluded given that its prompt component exceeds the total γ -ray flux (Fig. 6).

Acknowledgments

The authors would like to thank Carmelo Evoli, Ran Lu and Gabrijela Zaharijas for valuable discussions. PU acknowledges partial support from the European Union FP7 ITN INVISIBLES (Marie Curie Actions, PITN-GA-2011-289442).

-
- [1] C. Weniger (2012), 1204.2797.
 - [2] M. Su and D. P. Finkbeiner (2012), 1206.1616.
 - [3] M. Ackermann et al. (LAT Collaboration) (2012), 1205.2739.
 - [4] E. Tempel, A. Hektor, and M. Raidal (2012), 1205.1045.
 - [5] W. Buchmuller and M. Garny (2012), 1206.7056.
 - [6] A. Boyarsky, D. Malyshev, and O. Ruchayskiy (2012), 1205.4700.
 - [7] M. Cirelli, P. Panci, and P. D. Serpico, Nucl.Phys. **B840**, 284 (2010), 0912.0663.
 - [8] M. R. Buckley and D. Hooper (2012), 1205.6811.
 - [9] F. Aharonian, D. Khangulyan, and D. Malyshev (2012), 1207.0458.
 - [10] S. Profumo and T. Linden (2012), 1204.6047.
 - [11] K. Gorski, E. Hivon, A. Banday, B. Wandelt, F. Hansen, et al., Astrophys.J. **622**, 759 (2005), astro-ph/0409513.
 - [12] T. F.-L. Collaboration, Astrophys.J.Suppl. **199**, 31 (2012), 1108.1435.
 - [13] M. Su, T. R. Slatyer, and D. P. Finkbeiner, Astrophys.J. **724**, 1044 (2010), 1005.5480.
 - [14] G. Dobler, D. P. Finkbeiner, I. Cholis, T. R. Slatyer, and N. Weiner, Astrophys.J. **717**, 825 (2010), 0910.4583.
 - [15] G. Dobler, I. Cholis, and N. Weiner, Astrophys.J. **741**, 25 (2011), 1102.5095.
 - [16] A. A. Abdo, M. Ackermann, M. Ajello, A. Allafort, L. Baldini, J. Ballet, G. Barbiellini, D. Bastieri, K. Bechtol, R. Bellazzini, et al., Astrophys. J. **718**, 348 (2010).
 - [17] M. Ajello, A. Allafort, L. Baldini, J. Ballet, G. Barbiellini, et al., Astrophys.J. **744**, 80 (2012), 1109.3017.
 - [18] T. Bringmann, X. Huang, A. Ibarra, S. Vogl, and C. Weniger (2012), 1203.1312.
 - [19] C. Evoli, D. Gaggero, D. Grasso, and L. Maccione, JCAP **0810**, 018 (2008), 0807.4730.
 - [20] <http://www.desy.de/maccione/DRAGON/>.
 - [21] I. Cholis, M. Tavakoli, C. Evoli, L. Maccione, and P. Ullio, JCAP **1205**, 004 (2012), 1106.5073.
 - [22] M. Tavakoli (2012), Three-Dimensional Distribution of Atomic Hydrogen in the Milky Way.
 - [23] M. Tavakoli, I. Cholis, C. Evoli, and P. Ullio (2012), Diffuse Galactic Gamma Rays at intermediate and high latitudes. II. Constraints on the DM properties.
 - [24] I. A. Grenier, J.-M. Casandjian, and R. Terrier, Science **307**, 1292 (2005).
 - [25] T. F.-L. Collaboration (The Fermi-LAT Collaboration), Astrophys.J. **750**, 3 (2012), 1202.4039.
 - [26] A. Rajaraman, T. M. Tait, and D. Whiteson (2012), 1205.4723.
 - [27] R. Catena and P. Ullio, JCAP **1008**, 004 (2010), 0907.0018.
 - [28] P. Salucci, F. Nesti, G. Gentile, and C. Martins, Astron.Astrophys. **523**, A83 (2010), 1003.3101.
 - [29] T. Cohen, M. Lisanti, T. R. Slatyer, and J. G. Wacker (2012), 1207.0800.
 - [30] B. S. Acharya, G. Kane, P. Kumar, R. Lu, and B. Zheng (2012), 1205.5789.
 - [31] <http://fermi.gsfc.nasa.gov/ssc/data/analysis/scitools/>
 - [32] We check that changing the number of energy bins (between 25-35 bins) and their exact centers influences the limits on the continuous component only by $\simeq 1\%$ and the estimation of the best fit value for the line(s) by up to 30% which is within the 1σ stated uncertainty of [13] and [1] for the luminosity of the line. Our choice of 30 bins is made to include almost all the line signal in one bin while having a large number of bins with good statistics

for the continuous component.

[33] In [2] 16 logarithmically spaced energy bins were used to analyze the data between 80 and 200 GeV. That choice results in the bins being separated by a geometric factor

of 1.06. Based on that we take a 4% uncertainty in the energy which is more than half an energy bin in [2].